

Article

Plastid Phylogenetics, Biogeography, and Character Evolution of the Chinese Endemic Genus *Sinojackia* Hu

Xing Jian ^{1,*}, Yuliang Wang ², Qiang Li ³  and Yongmei Miao ^{2,*}¹ College of Architecture, Anhui Science and Technology University, Bengbu 233000, China² College of Life and Health Sciences, Anhui Science and Technology University, Fengyang 233100, China; wangyul@ahstu.edu.cn³ Co-Innovation Center for Sustainable Forestry in Southern China, College of Life Sciences, Nanjing Forestry University, Nanjing 210037, China; liqiang9503@163.com

* Correspondence: jianx@ahstu.edu.cn (X.J.); miaoym@ahstu.edu.cn (Y.M.)

Abstract: *Sinojackia* Hu. comprises five to eight Chinese endemic species with high ornamental and medicinal value. However, the generic limits, interspecific relationships and evolutionary history of the genus remain unresolved. In this study, we newly sequenced three plastomes of *S. oblongicarpa* and compared them with those of the other congeneric species to explore the taxonomic delimitation of the species and the evolutionary history of the genus. The plastome structure of *Sinojackia* species was extremely conserved in terms of number of genes, sequence length, and GC content. The codon usage patterns revealed that natural selection may be the main factor shaping codon usage bias. Our phylogenetic tree shows that *Sinojackia* is monophyletic and can be divided into two clades. *Sinojackia oblongicarpa* as a distinct species is supported for it is distantly related to *S. sarcocarpa*. The evolutionary analysis of morphological features indicates that the woody mesocarp is an ancestral feature. *Sinojackia* originated in central Southeast China during the early Miocene. In this period, it experienced elevated diversification and migrated from central Southeast China to the Hunan Province and the Sichuan Province with the development of the Asian monsoon and East Asian flora. Glacial–interglacial interactions with the monsoon climate may provide favorable expansion conditions for *Sinojackia* on a small scale.

Keywords: *Sinojackia*; plastome; species delimitation; evolutionary history

Citation: Jian, X.; Wang, Y.; Li, Q.; Miao, Y. Plastid Phylogenetics, Biogeography, and Character Evolution of the Chinese Endemic Genus *Sinojackia* Hu. *Diversity* **2024**, *16*, 305. <https://doi.org/10.3390/d16050305>

Academic Editor: Mario A. Pagnotta

Received: 6 May 2024
Revised: 16 May 2024
Accepted: 16 May 2024
Published: 18 May 2024



Copyright: © 2024 by the authors. Licensee MDPI, Basel, Switzerland. This article is an open access article distributed under the terms and conditions of the Creative Commons Attribution (CC BY) license (<https://creativecommons.org/licenses/by/4.0/>).

1. Introduction

The data for phylogenetic datasets have historically utilized single or a few DNA fragments (i.e., cpDNA fragments and nrDNA), limiting the information that is available in a complete genomic dataset [1–5]. However, many nuclear loci as well as plastid loci have undergone random noise (i.e., positive selection) [6], thus using these positively selected sites may greatly impact phylogenetic signals and produce discordant phylogenetic trees. Plastomes possess large numbers of loci and are less subject to selective effects, generally resulting in improved resolution compared to traditional multilocus plastid phylogenies [7,8]. For this reason, plastomes have been widely utilized for phylogenetic reconstruction, ancestral state reconstruction, species delimitation, divergence time estimation, and inference of the biogeographic origins of angiosperms [9–12]. Beyond being utilized for phylogenetic and biogeographic analysis, comparing the content and structure of plastomes can help further understand species evolution.

Sinojackia Hu is an endemic genus of Styracaceae in China. It comprises approximately five to eight species of shrubs and trees distributed in Central, Southern, and Southwest China [13–17]. Species of *Sinojackia* are valued as ornamental garden plants for their white fragrant flowers and unique, heavy, hammer-like fruits [18], also valued for their medicinal properties [19]. Most of the species in *Sinojackia* are endangered or threatened because of their small population size, deforestation, and other manmade activities [20–23].

The genus was established by Hu with one species *Sinojackia xylocarpa* Hu [24]. Since then, seven new names have been described (*S. dolichocarpa* [25], *S. huangmeiensis* J. W. Ge and X. H. Yao [16], *S. microcarpa* Tao Chen bis and G. Y. Li [26], *S. oblongicarpa* Tao Chen bis and T. R. Cao [27], *S. rehderiana* Hu [28], *S. sarcocarpa* L. Q. Luo [29], *S. xylocarpa* var. *Leshanensis* L. Q. Luo [30]), and one species, *Pterostyrax henryi* Dümmer., was transferred to the genus [31]. Nevertheless, the generic limits and the circumscriptions of the *Sinojackia* species remain unclear, as fruits of these species are morphologically variable across their geographical ranges [14,15,32]. The monotypic genus *Changiostyrax* was split from *Sinojackia* to accommodate *C. dolichocarpus* based on the facts that the trunk has no spines, the buds have scales, and flowers are four-merous [33]. The taxonomic independence of *Changiostyrax* from *Sinojackia* is supported by both morphological [33,34] and molecular studies [32,35,36]. However, Hwang and Grimes (1996) recognized five species of *Sinojackia* in 'Flora of China' and retained *S. dolichocarpa* in the genus [13]. *Sinojackia oblongicarpa* C. T. Chen and T. R. Cao was reduced to a synonym of *sarcocarpa* by Luo (2005) [14]. Subsequently, *S. rehderiana* and *S. huangmeiensis* were reduced to synonyms of *S. xylocarpa* by Luo and Luo (2011) [15]. Furthermore, *Sinojackia henryi* (Dummer) Merr. has disappeared for nearly 70 years without collection records.

Previous molecular phylogenetic analyses revealed that *Sinojackia* is monophyletic and can be resolved into two major clades with generally weak bootstrap support in interspecific relationships [32,37]. However, the phylogenetic relationships of the species are inconsistent in different studies, for example, *S. microcarpa*, *S. oblongicarpa*, *S. sarcocarpa*, and *S. huangmeiensis* formed a monophyletic clade, and *S. xylocarpa* and *S. rehderiana* formed another clade according to Yao (2008) based on the combined ITS and *psbA-trnH* analysis [32]. However, *S. xylocarpa* formed a sister group with the *S. sarcocarpa* and *S. oblongicarpa*, while *S. huangmeiensis* and *S. rehderiana* clustered with *S. microcarpa* in the results of Fan (2015) [37]. The two clades resolved by Yao (2008) were strongly supported by genome-based studies [20,36,38,39]. However, the taxonomic position and phylogenetic relationship of *S. oblongicarpa* is still unclear for it is not sampled in previous genome-based studies.

To improve our understanding of the evolution of *Sinojackia*, benefit taxonomic and applied research, and support conservation efforts, a robust phylogenetic framework of the genus was reconstructed based on the plastomes of three newly sequenced individuals of *S. oblongicarpa* and 14 previously published plastomes. The aims of this study are to (1) characterize and compare the plastid genome of *Sinojackia*, (2) resolve evolutionary relationships among species in the genus, and (3) infer the timings of the diversification and trace the biogeographical history.

2. Materials and Methods

2.1. Sample Collection, DNA Extraction, Sequencing, and Assembly

In this study, fresh leaf material from three wild individuals of *S. oblongicarpa* individuals was collected from a wild population located in Huaihua city, Hunan Province (27.6563 E, 109.8705 N) (Figure 1), and preserved in silica gel and stored in a refrigerator at -80°C . The total DNA was extracted using the modified cetyl trimethyl ammonium bromide (CTAB) method following the manufacturer's instructions [40]. Illumina sequencing libraries were generated on the Illumina NovaSeq platform at Personalbio (Shanghai, China), with a 150 bp paired-end (insert size of 400 bp) strategy. High-quality reads were obtained from the raw data after filtering by using fastP v0.15.0 (-n 10 and -q 15) [41]. Then, de novo assembly of the clean data was performed by using the GetOrganelle v1.7.5.0 pipeline [42] with k-mers 21, 45, 65, 85, and 105. Bandage was used to confirm whether the plastomes were a closed loop [43].



Figure 1. Distribution and sampling of *Sinojackia*.

2.2. Plastome Annotation

The annotation of three plastomes of *S. oblongicarpa* was performed on the online program CPGAVAS2 (<http://47.96.249.172:16019/analyzer/home>, accessed on 5 December 2023) [44] and the GeSeq tool (<https://chlorobox.mpimp-golm.mpg.de/geseq.html>, accessed on 14 December 2023), with the published plastomes of the other five species of *Sinojackia* as a reference [45]. Assembly errors were identified and manually resolved using Sequin software. The circular diagram of the fully annotated plastomes was drawn by OrganellarGenomeDRAW (OGDRAW) [46].

2.3. Comparative Analyses of Plastomes

Comparative genomic analyses were carried out among 17 accessions of *Sinojackia* plastomes. Multiple sequence alignments were performed on the online tool MAFFT [47] with the default parameters. To identify sequence divergence hotspot regions, the nucleotide diversity (π) was calculated using DnaSP v6 [48]. The plastomes were compared using the online tool mVISTA (<https://genome.lbl.gov/vista/mvista/submit.shtml>, accessed on 20 December 2023), with a shuffle-LAGAN model and *S. oblongicarpa* as a reference.

2.4. Codon Usage Pattern Analyses

The following principles were used for the subsequent analysis of the protein-coding sequences (CDSs) of the compared plant species: (1) excluding sequence lengths less than 300 bp; and (2) deleting one of the multicopy genes.

Generally, the value of the ENC (effective number of codon) ranges from 20 to 61. The ENC value was less than 35, indicating that significant bias occurred in the codon usage pattern [49]. The R software package CodonW 1.4.2 was applied to calculate the ENC value. The frequency of GC content, including GC1 (at the first position), GC2 (at the second position), and GC3 (at the third position) was calculated in the online program CUSP (<http://emboss.toulouse.inra.fr/cgi-bin/emboss/cusp>, accessed on 20 December 2023).

Codon usage bias is shaped by the correlation between GC12 (average of GC1 and GC2) and GC3. When the correlation between the two is high, mutations are the main factor affecting codon bias. In contrast, when the two are not significantly correlated, natural

selection dominates the codon usage bias. Furthermore, the slope of the regression curve was close to 0, indicating that natural selection dominated the codon usage [50].

An ENC plot was used to measure the value of ENC against GC3. When all genes were on the standard curve, there was no codon usage bias. When the gene is above the curve, mutation pressure dominates codon bias; otherwise, natural selection dominates [51].

PR2 (parity rule 2) is an effective method to evaluate the degree to which codons are affected by natural selection and mutation pressure. AU bias [$A3/(A3 + U3)$] and GC bias [$G3/(G3 + C3)$] act as the coordinate axes. When the frequency is $A = T$ and $G = C$, all the genes will be located in the center of the coordinate axis, and the effect of mutation pressure and natural selection are equal. When the site deviates from the center, mutation, selection, or both affect codon usage patterns [52].

2.5. Phylogenetic Analyses

To determine the phylogenetic relationship within *Sinojackia*, 14 published plastome sequences of *Sinojackia*, 7 plastome sequences of *Styracaceae*, and 1 outgroup (*Symplocos tanakana* NC_058289) were downloaded from the NCBI database. A total of 25 accessions were used for phylogenetic analyses. Multiple sequence alignment was performed on the online program MAFFT. PhyloSuit [53] was used to move the gap with the default set. The maximum likelihood (ML) method was used to construct a phylogenetic tree in IQTREE 2 [54], with 1000 bootstrap replications. The best-fitting model was K3Pu+F+R6, which was identified by ModelFinder.

2.6. Divergence Time Estimate

The divergence time within *Sinojackia* was estimated in the program BEAST v2.6.3 [55], with an uncorrelated lognormal relaxed molecular clock model. The aligned plastomes were used as an input file in BEAUti, in which the GTR model and Yule speciation tree prior were applied. The Bayesian analysis had a chain length of 100 million generations with sampling every 10,000 generations. Trace was used to assess the effective sample size of each parameter ($ESS > 200$). After discarding 25% of trees as burn-in, the samples were summarized in a maximum-clade tree in TreeAnnotator with the mean node heights.

Two fossils and one secondary calibration were applied to time-calibrate the phylogenetic tree of *Sinojackia*. The fossil record of *Styrax elegans* (56–47.8 Ma) [56] was used as the stem age of *Styrax* (A) and was set to 56.0 Ma (95% highest posterior density (HPD) 65.1–48.7 Ma). The fossil record of *Halesia reticulata* (37.2–33.9 Ma) was set as the second calibration (B) (mean 35.0 Ma, 95% HPD = 37.5–32.5 Ma) [57]. One secondary calibration point derived from previous work was used to set the stem age of *Sinojackia* [58,59]. The third calibration point (C) had the following parameters: mean = 23.0 Ma; 95% HPD = 27.9–18.1 Ma.

2.7. Biogeographic Analyses

The geographical distribution of *Sinojackia* was obtained from the National Plant Specimen Resource Center (<http://www.nsii.org.cn/2017/home.php>, accessed on 18 December 2023) and the literature records [60] (Figure 1). Southwest China is one of the hotspots of biodiversity in China, and we mainly tested whether the genus *Sinojackia* had spread from Southwest to Southeast China. Therefore, three major geographic areas were defined: (A) Sichuan Province; (B) Hunan Province; and (C) central Southeast China region (Hubei, Anhui, Jiangsu, Zhejiang, Jiangxi, Guangdong). Considering that there may be multiple origins, the Bayesian binary MCMC method (BBM), which was implemented in the software RASP v4.3, was applied to reconstruct the biogeographic history of *Sinojackia* [61].

2.8. Ancestor State Analyses

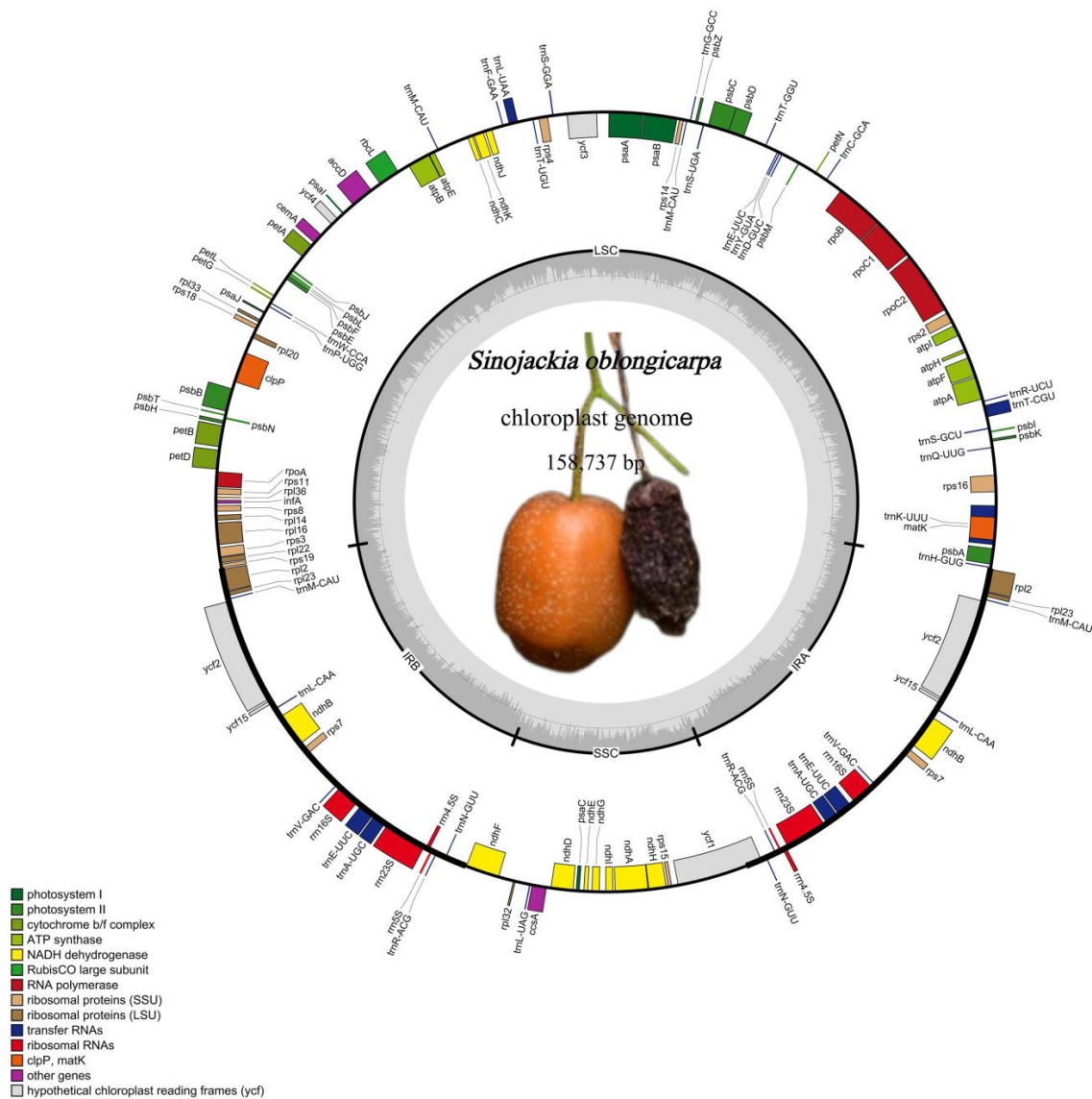
To understand character evolution within *Sinojackia*, four traits were selected based on the type of mesocarp: mesocarp wood, mesocarp undeveloped, mesocarp fleshy, and mesocarp spongy. The topological structure of the tree was derived from the results of

IQTREE. The ancestral characters of *Sinojackia* were inferred using the online program PastML [62] with the MAP (maximum a posteriori) method and F81 evolution models.

3. Results

3.1. Characterization of the Complete Plastome of *S. oblongicarpa* and Comparison with Its Congeneric Species

Approximately 8.63 GB (*S. oblongicarpa* OQ985173) to 10.6 GB (*S. oblongicarpa* OQ985171) of the NGS clean data were generated for each sample. Three *S. oblongicarpa* plastomes were newly generated during the current study. All the three plastomes exhibited quadripartite structures with a large single-copy (LSC) region (87,995 bp), a small single-copy (SSC) region (18,562 bp), and two inverted repeat IR (IRa and IRb) regions (26,090 bp). All the three plastomes were 158,737 bp in length and showed identical sequences. The GC content of the plastome accounted for 37.3%. All plastomes had the same 79 protein-coding genes, 30 transfer RNA (tRNA) genes, and 4 ribosomal RNA (rRNA) genes for a total of 113 unique genes (Figure 2). Furthermore, two copies of *ndhB*, *rpl2*, *rpl23*, *rps7*, *ycf2*, and *ycf15* were detected in the plastomes.



158,758 bp in length, respectively. The total length of the *Sinojackia* plastomes varied by only 35 bp, revealing a high extent of similarity. The largest LSC region was found in *S. oblongicarpa* (87,955 bp) and the smallest LSC was in *S. huangmeiensis* (88,023 bp). The SSC region ranged from 18,551 bp (*S. xylocarpa*) to 18,586 bp (*S. rehderiana*). The IR regions were found in a similar range between 26,090 bp (*S. oblongicarpa*, *S. xylocarpa*, *S. sarcocarpa*, and *S. huangmeiensis*) and 26,100 bp (*S. rehderiana*). All the plastomes had the same gene content and gene number. All the plastomes possessed equal GC contents, accounting for 37.3% (Table 1).

Table 1. Comparative analysis of general characteristics of the plastomes.

Species	Length (bp)	LSC (bp)	SSC (bp)	IR (bp)	GC Content (%)	Number of Gene	CDS	tRNA	rRNA
<i>S. oblongicarpa</i>	158,737	87,955	18,562	26,090	37.3	113	79	30	4
<i>S. xylocarpa</i>	158,725	87,994	18,551	26,090	37.3	113	79	30	4
<i>S. sarcocarpa</i>	158,737	88,002	18,555	26,090	37.3	113	79	30	4
<i>S. rehderiana</i>	158,760	87,974	18,586	26,100	37.3	113	79	30	4
<i>S. microcarpa</i>	158,739	88,002	18,553	26,092	37.3	113	79	30	4
<i>S. huangmeiensis</i>	158,758	88,023	15,555	26,090	37.3	113	79	30	4

3.2. Comparative Genomic Analysis and Divergence Hotspot Regions

Pairwise comparisons of the divergent regions within the *Sinojackia* plastome sequences revealed that they were highly conserved across the plastome sequences (Figure 3). A slight variation was still detected in the *Sinojackia* plastome, and most of the variation was present in non-coding regions. Among these variation regions, the non-conserved regions in the protein-coding regions were detected in the *rpl32* and *ycf1* genes. The non-conserved regions in the non-coding regions all were intergenic spacers: *atpA-atpF*, *trnT-GUU-psbD*, and *ycf15-trnL-CAA*.

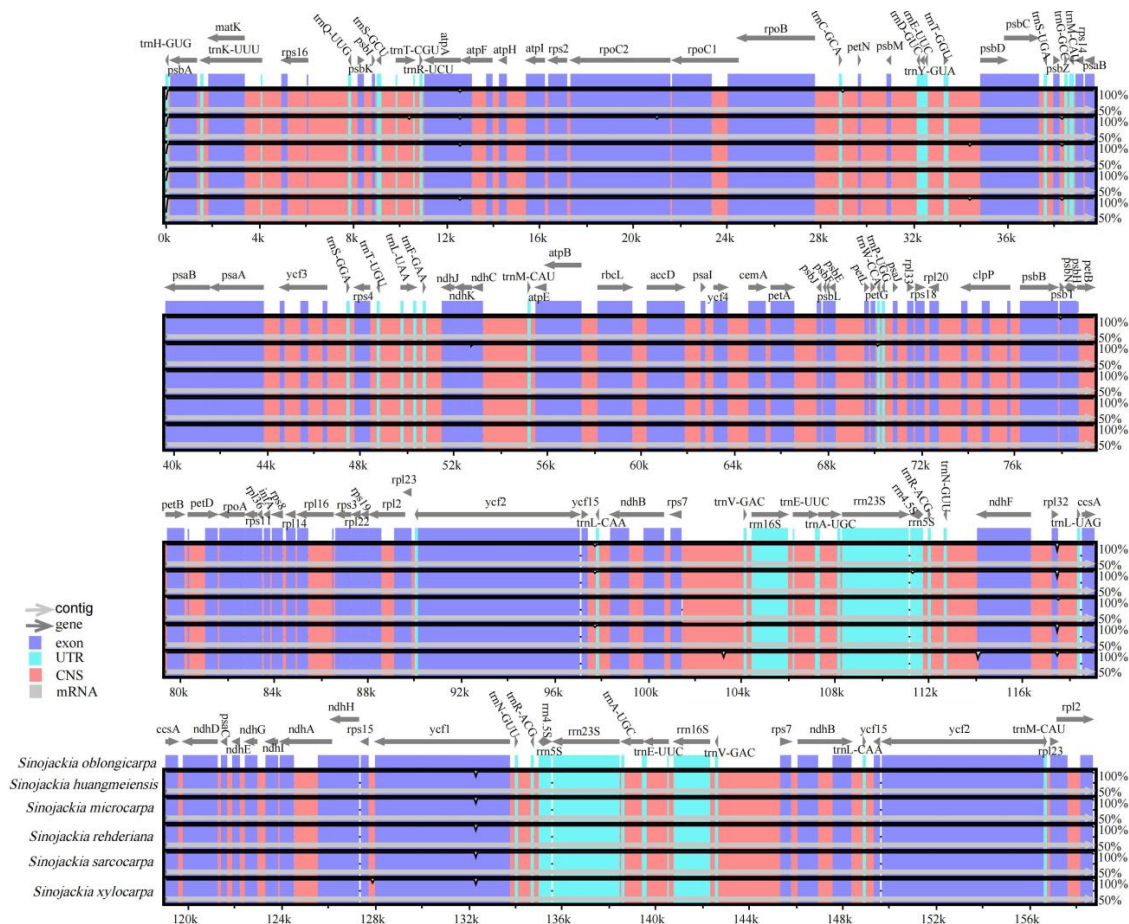


Figure 3. Comparison of *Sinojackia* plastome genomes using mVISTA. Blue represents coding regions, green represents RNA regions, and red represents non-coding regions.

The nucleotide diversity (P_i) values were calculated within 400 bp windows to identify sequence divergence hotspots (Figure 4). The nucleotide diversity of the aligned plastomes was compared across all taxa and varied from 0 to 0.01. The SSC region possessed relatively high variation compared with the LSC and IR regions. The nucleotide diversity values of *rpl32* and *rpl32-trnL* were the highest, which were 0.01 and 0.009, respectively.

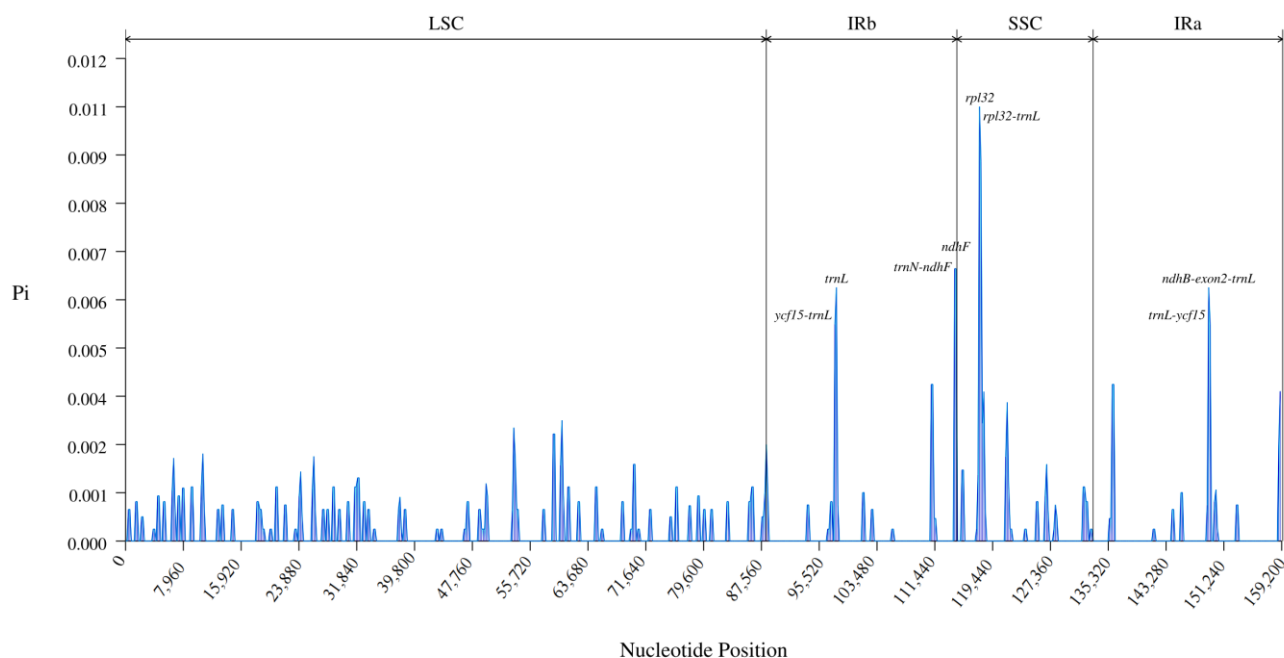


Figure 4. Nucleotide diversity (P_i) of 17 *Sinojackia* plastomes.

3.3. Codon Usage Pattern Analyses

Neutral-Plot, ENC-Plot, and PR2-Plot analyses were applied in *Sinojackia* species. All the species showed a similar codon usage pattern (Figure S1–S5). In Figure 5, the codon preference pattern of *S. oblongicarpa* is illustrated.

Generally, the value of ENC ranges from 20 to 61. Our results show that the majority of genes possessed ENC values greater than 35, indicating that a relatively weak codon bias exists in *Sinojackia*. The vast majority of points were distributed below the standard curve, which indicated that natural selection and other factors may dominate the codon usage pattern in the genus *Sinojackia*. The ENC ratios of the majority of chloroplast genes were distributed in the range of 0.05–0.15. These results indicated that natural selection dominated the codon usage bias in *Sinojackia* plastomes.

The correlation between GC12 and GC3 was calculated, and our results showed that the adjusted R^2 was -0.058 . There was no significant correlation between GC12 and GC3; therefore, the codon usage was mainly affected by natural selection. The slope of the regression line was 0.156, indicating that mutation pressure accounted for 15.6%. Therefore, mutation and natural selection are both factors affecting the codon bias, but natural selection is the main one.

The frequency of A, T, C, and G used in GC3 was calculated. When all points are distributed at the center, indicating that $A = T$ and $G = C$, the codon is unbiased. In our present results, all the genes appeared in the lower right corner of the graph. This phenomenon indicates that the frequency of use of A and C was lower than that of G and T. Extremely few genes appeared at the center, indicating that natural selection interacting with mutation pressure plays a crucial role in shaping the codon usage patterns.

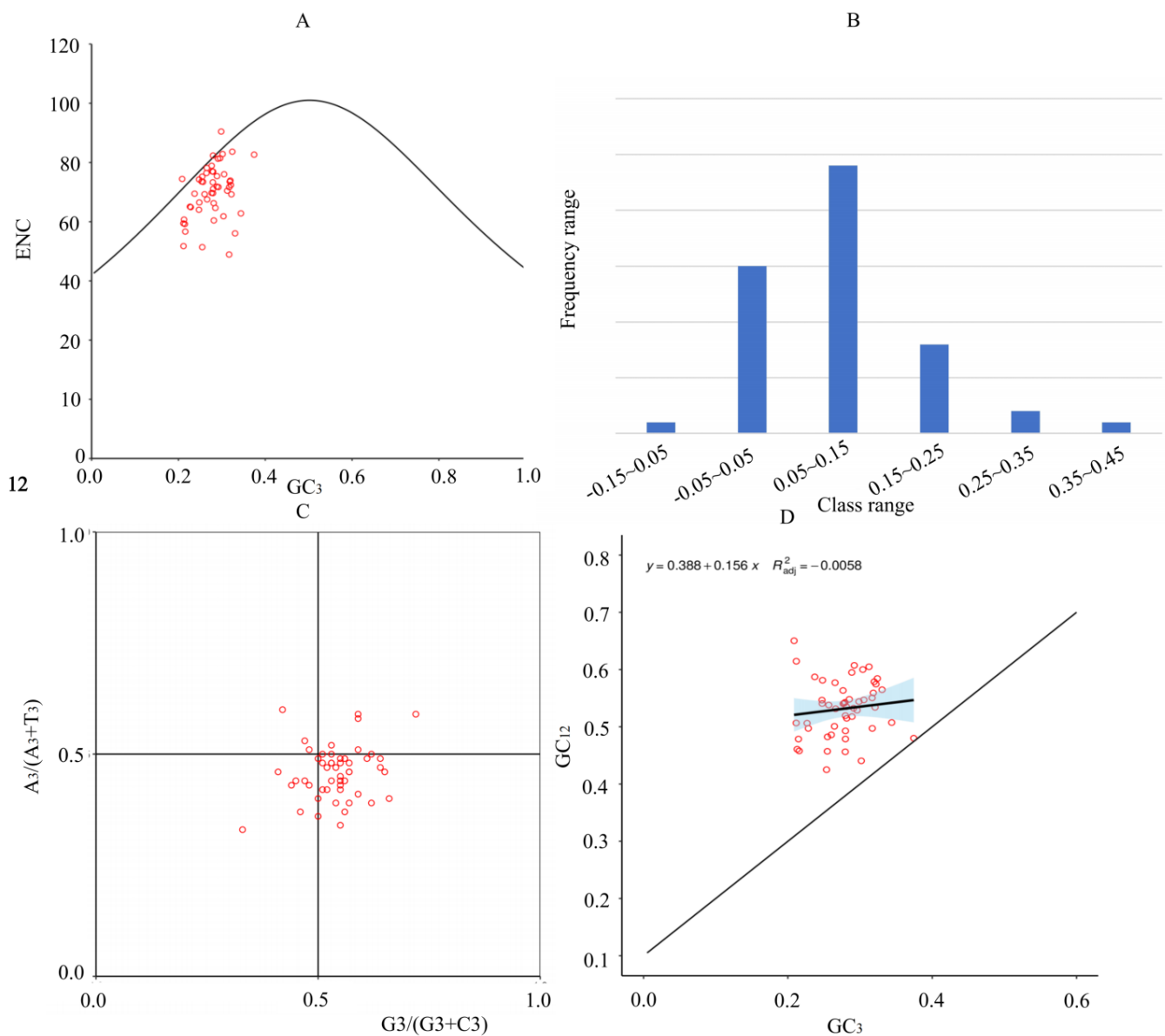


Figure 5. Codon usage bias analyses of *S. oblongicarpa*. (A) ENC plot analyses show the relationship between ENC and GC₃; (B) frequency distributions of the ENC ratio; (C) PR2-bias plot; (D) neutrality plot.

3.4. Phylogenetic Analyses

The reconstructed phylogeny from the complete plastome received high bootstrap support values (the vast majority of the nodes scored more than 90%) (Figure 6). *Sinojackia* was well supported as a monophyletic group and sister to *Pterostyrax*. *Sinojackia* clustered into two main clades (Clade A and Clade B) with high bootstrap values (100%). Clade A contained three species, including *S. microcarpa*, *S. sarcocarpa*, and *S. huangmeiensis*. Clade B comprised *S. xylocarpa*, *S. rehderiana*, and *S. oblongicarpa*. Three individuals of *S. sarcocarpa* were clustered into one clade sister to *S. huangmeiensis*, with a bootstrap value of 100%. Individuals of *S. xylocarpa* and *S. rehderiana* were mixed together. *S. oblongicarpa* was a sister to (*S. xylocarpa* + *S. rehderiana*) with strong support (100%).

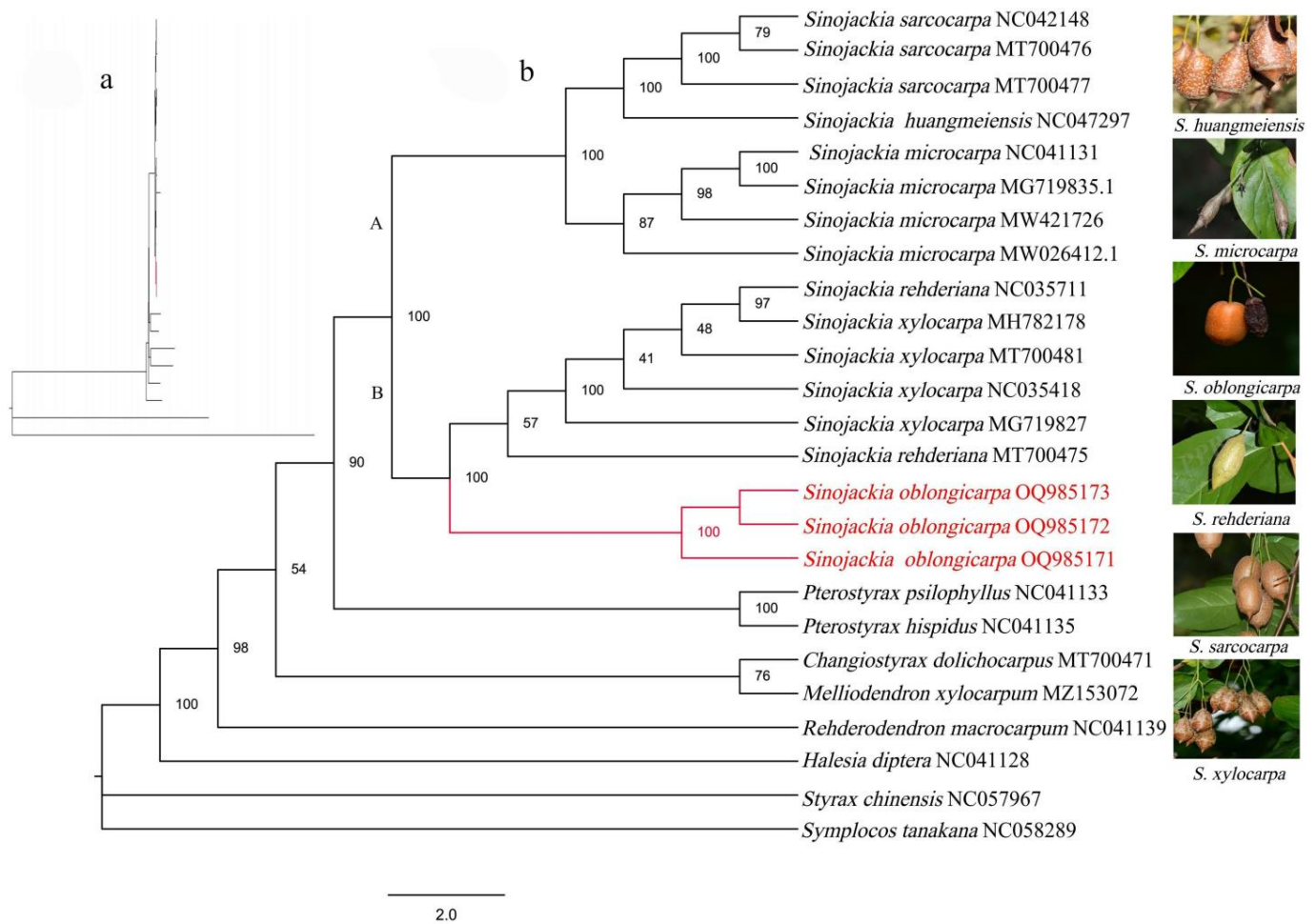


Figure 6. Maximum-likelihood (ML) phylogram (a) and cladogram (b) of *Sinojackia* based on the whole-plastome sequence. The red font represents the newly sequenced species.

3.5. Evolutionary History Analyses

The phylogenetic tree inferred by IQTREE was used to analyze the evolution of fruit type in the genus *Sinojackia* (Figure 7). Our results show that the ancestral state of fruit type in this genus was probably mesocarp woody (*S. xylocarpa*, *S. rehderiana*), with mesocarp undeveloped and fleshy possibly deriving from it. Mesocarp spongy may be derived from fleshy. The multiple occurrences of mesocarp fleshy may be the result of parallel evolution.

Divergence time estimates for the genus *Sinojackia* were performed based on the complete plastid genome (Figure 8); the effective sample size was above 200 for all parameters. *Sinojackia* and its sister diverged in the early Miocene (20.89 Ma, 95% highest posterior density (HPD), 16.04–25.88 Ma). The split between Clade A and Clade B was dated to 14.50 Ma (95% HPD, 7.01–21.33 Ma). The time of the *S. microcarpa* and (*S. sarcocarpa* + *S. huangmeiensis*) split was at 9.44 Ma (05% HPD, 3.01–16.25 Ma). The diversification of *S. microcarpa* was at approximately 5.04 Ma (95% HPD, 0.50–10.76 Ma). *S. oblongicarpa* occurred at 5.57 Ma (0.19–12.86 Ma).

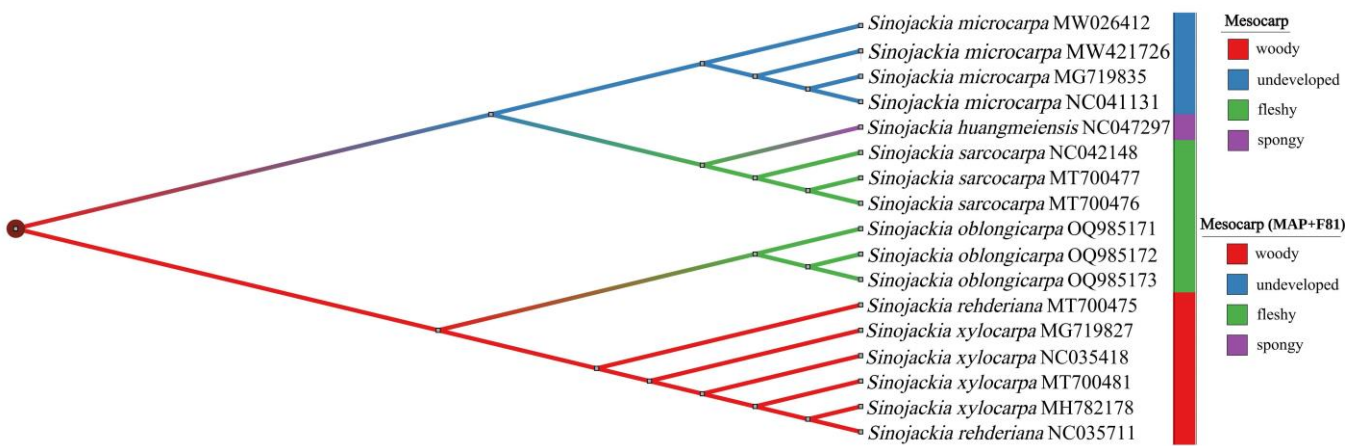


Figure 7. Inference of ancestral state of fruit in *Sinojackia*. The colors of the topological structure lines represent the possible traits of ancestors.

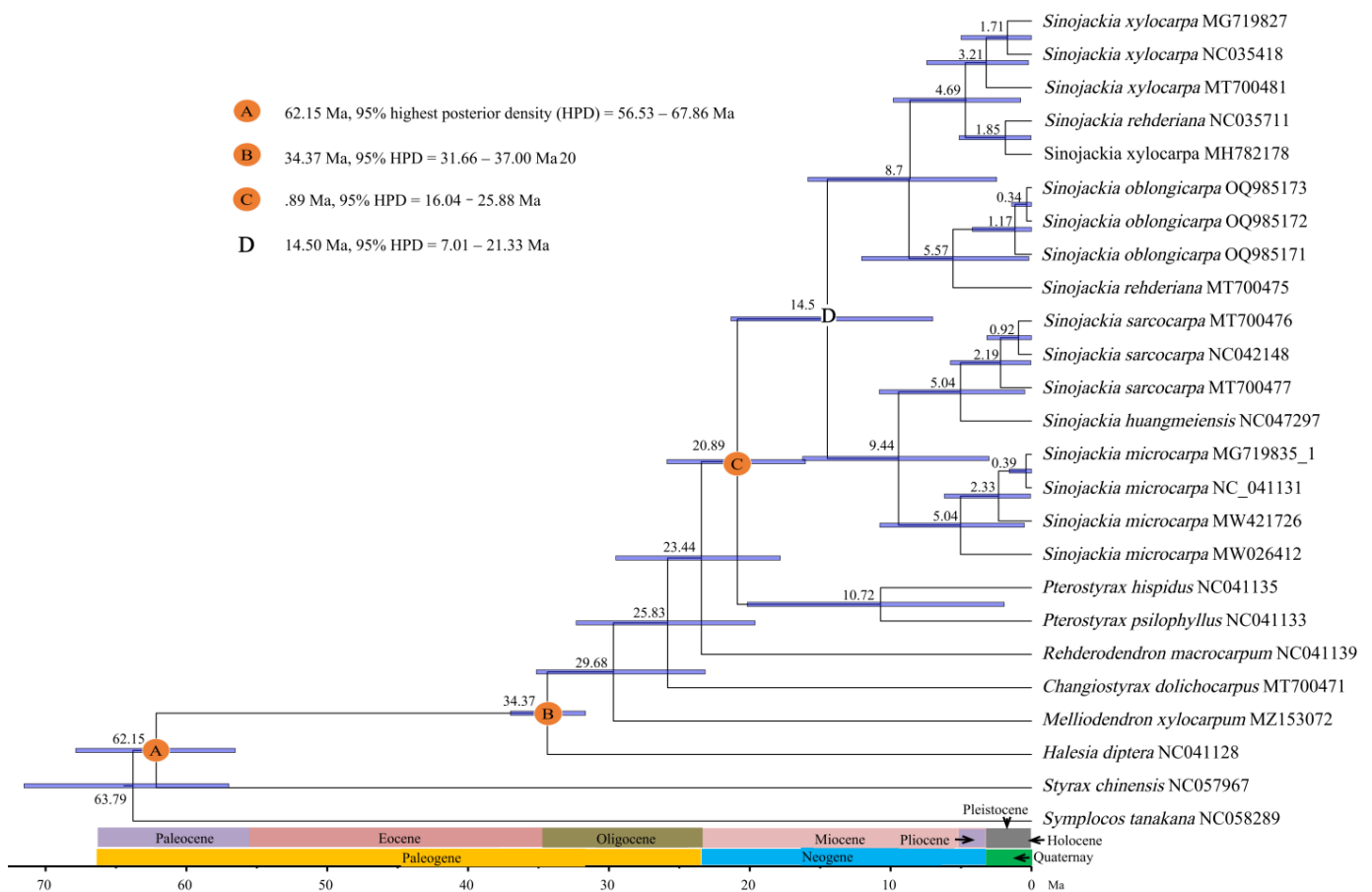


Figure 8. Divergence time of *Sinojackia* estimated by BEAST based on the whole plastome. A, B, and C indicate fossil calibration points.

The ancestral area reconstruction implied that central Southeast China (C) was the most probable ancestral area for *Sinojackia*. Subsequently, a dispersal event occurred from central Southeast China (C) to Hunan Province (B) and Sichuan Province (A) (Figure 9a). We also calculated the trend of the dispersal, variation, and extinction events over time. The results show that no extinction events have occurred, and the rates of dispersal and variation are the same (Figure 9b).

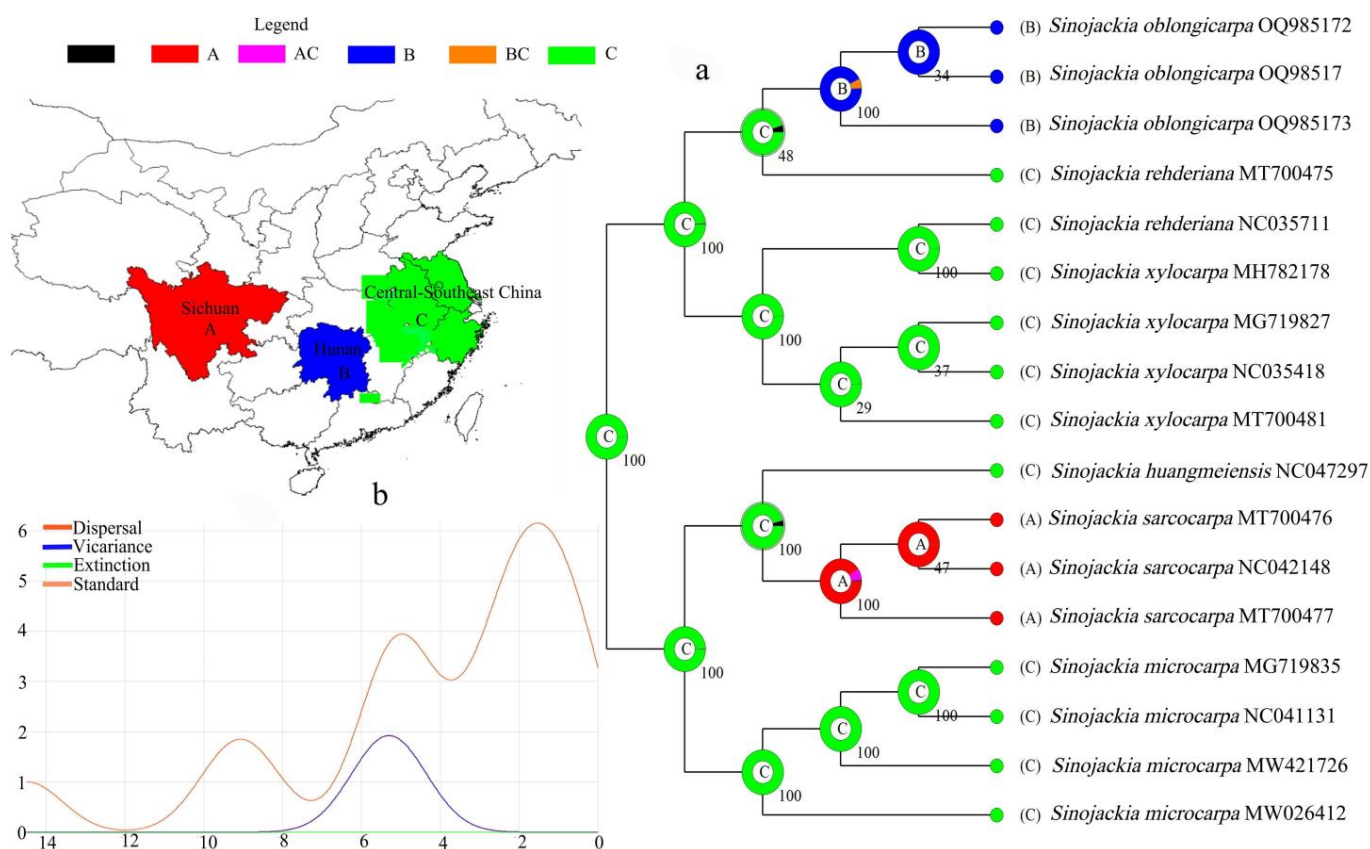


Figure 9. Biogeographic results of *Sinojackia*. (a) Displays the possible origins of ancestors; (b) displays the rates of dispersal and variation.

4. Discussion

4.1. Plastome Structure and Sequence Variation

Comparative plastome analysis among species of *Sinojackia* has been carried out in previous studies [20,36]. However, these previous studies included only three to five species, limiting a comprehensive understanding of the plastome evolution of this genus. Our study includes all known extant species (except *S. henryi*, which may be extinct or a synonym) and compares the structure and content of the plastome, which will greatly enrich our understanding of the evolution of the Chinese endemic genus *Sinojackia*. In the present study, the plastomes of *Sinojackia* were highly conserved in overall structure, gene numbers, content, and order. They were similar in size and gene content to the previously reported plastomes of Styracaceae species [36]. The total size of the plastomes ranged from 158,725 bp to 158,760 bp. Such a slight variation was more conservative than that in previous studies of other angiosperm plant lineages [63,64], and even smaller than the difference in the plastome at the intraspecific level of some taxa, such as *Toxicodendron vernicifluum* (1322 bp) [65] and *Primula obconica* subsp. *obconica* (444 bp) [66]. The length of the LSC region was greater than that of the SSC and IR regions. Consistent with previous results [67], our results demonstrate that variation in the LSC region is primarily responsible for triggering genomic size variations. Sequences with a higher GC content are more stable and have lower mutation rates. The plastome possessed GC contents ranging from 20.46% to 57.66%, and the average GC content was 36.82% [68]. The GC content of *Sinojackia* accounted for 37.3%, exceeding the average level of GC content.

Almost no sequence variation was detected between *S. oblongicarpa* and its congeneric species. This may result from the fact that *Sinojackia* were distributed in low-elevation mountains and were less affected by climate fluctuations. Therefore, the interspecific genetic diversification has been maintained at a relatively low level. Generally, high-variation regions are used as potential molecular markers for interpreting phylogenetic relationships

in taxonomically problematic plant taxa [69]. However, the pi value of all regions was less than or equal to 0.01, indicating that chloroplast fragments may not be suitable as molecular markers in this genus. In fact, a previous phylogenetic tree based on chloroplast markers received lower bootstrap values in this genus [32]. Therefore, we suggest reconstructing the phylogenetic tree of land plants based on whole-chloroplast genome data, especially in the groups with very similar morphological characteristics.

4.2. Analysis of Factors Influencing Codon Bias

Codon usage bias is a widespread phenomenon across species and among functionally related genes and within a single gene [70,71]. Extensive research has been performed on codon usage bias in many plant groups, such as Rosales species [72] and *Epimedium* [73]. Natural selection and mutation pressure are two main biological factors in shaping codon usage bias [74,75]. In addition to being affected by these two biological factors, the codon usage bias is affected by many other factors, such as translation (selection for optimized translation), gene expression, rate of evolution, secondary structure of DNA, nucleotide composition, protein length, and environmental conditions [70,76,77]. In the present study, the Neutral-Plot, ENC-Plot, and PR2-Plot analyses were performed to investigate the codon usage pattern in *Sinojackia*. All the species showed similar results in codon usage pattern. The codon bias in some plastomes of the species was mainly affected by mutation pressure, such as in the genus *Quercus* [78] and *Coffea arabica* [79]. In other species, such as the genus *Gynostemma*, natural selection played a major role in shaping codon usage bias [80]. In *Sinojackia* plastomes, natural selection interacted with mutation pressure playing a crucial role in shaping the codon usage pattern, but natural selection was the primary driver of the codon usage in the *Sinojackia* plastomes.

4.3. Interspecific Phylogenetic Relationships

A robust phylogenetic framework is important for resolving the circumscription of the genus *Sinojackia* and for investigating evolutionary patterns and processes. Our ML phylogeny received strong support at most nodes of the tree. *Sinojackia* was well supported as a monophyletic group and sister to *Pterostyrax* in the current study, in agreement with previous phylogenetic analyses [35,36]. Two main clades were strongly supported in our results, but the systematic placement of *S. oblongicarpa* leads to contradictions between our results and previous research [32]. Yao et al. (2008) utilized several barcodes, including ITS, *psbA-trnH*, and seven microsatellite loci, to assess the phylogenetic relationship within *Sinojackia*, supported that *S. oblongicarpa* were sister to *S. microcarpa*, and formed one clade with *S. sarcocarpa* and *S. huangmeiensis*. However, all the branch nodes received an extremely low bootstrap rate within *Sinojackia* (<50%). The topological structure of our phylogenetic tree is consistent with that in previous studies based on plastomes [20,35,36,38,39] and resulted in well-resolved and highly supported phylogenies. We are convinced that our results have better interpretation ability.

S. oblongicarpa differs from *S. sarcocarpa* in its shrubby habit, smaller flowers (1.2–1.5 cm long), and oblong fruits [27]. *S. huangmeiensis* can be distinguished from *S. xylocarpa* by its smaller flowers, broad ovate petals, smaller and gray-brown fruits with a papillate short beak [23]. Previous research implied that the weight of *S. oblongicarpa* is related to environmental competition, and the size of its flowers and the shape of its fruits are within the variation range of *S. sarcocarpa*; therefore, *S. oblongicarpa* was retreated as a synonymy of *S. sarcocarpa* [14]. Subsequently, *S. rehderiana* and *S. huangmeiensis* were retreated as a synonym of *S. xylocarpa* based on morphological characters [15]. This was inconsistent with our phylogenetic tree, in which *S. oblongicarpa* was close to (*S. xylocarpa* + *S. rehderiana*) and formed distant phylogenetic relationships with *S. sarcocarpa*. Evidence from the rDNA-ITS phylogenetic tree also demonstrated that *S. oblongicarpa* and *S. sarcocarpa* were not sister species [37]. Therefore, we suggest that *S. oblongicarpa* should be treated as an independent species. In terms of the taxonomy of *S. huangmeiensis*, both our results and previous molecular phylogenetic analyses reveal that *S. huangmeiensis* formed a distant phylogenetic relationship with *S. xylocarpa* [20]. The taxonomic

relationship between *S. rehderiana* and *S. xylocarpa* remains a challenge. Hybridization tests were successful in ex situ collections between *S. rehderiana* and *S. xylocarpa* [81], proving that gene flow may weaken the boundary between these two species. In general, geographical isolation may hinder the occurrence of interspecific hybridization events. The distribution of *Sinojackia* is highly fragmented, enhancing the difficulty of gene flow. Therefore, some scholars have speculated that *Sinojackia* may have had a wide distribution range in the past, and habitat destruction and self-propagation constraints may have resulted in the fragmented distribution pattern that is seen today [32]. Thus, extensive taxon sampling and molecular characterization are essential in further taxonomic studies between *S. rehderiana* and *S. xylocarpa*.

4.4. Evolutionary History Analysis

Narrow geographical distribution, habitat destruction, and seed germination limitations pose great challenges to the survival of the genus *Sinojackia*. The permeability of the endosperm and the mechanical barrier of the pericarp play an important role in seed dormancy [82,83]. Our result results demonstrated that mesocarp woody is probably an ancestral state in the genus *Sinojackia*. Actually, mesocarp woody is the fruit type with the most variable shapes and the widest distributed fruit type compared to the other three fruit types. Mesocarp woody may hinder the permeability of the endosperm, thus prolonging the germination time of seeds. The types mesocarp fleshy and mesocarp free may be more evolved, owing to their increased endosperm permeability and reduced mechanical hindrance in seed germination.

In our chronogram, Symplocaceae and Styracaceae split around 63.45 Ma (95% HPD: 56.98–71.93 Ma). This is congruent with the result of Dexter et al. [84] and Li et al. [85]. The age of *Styrax* emerged at 62.15 (95% HPD: 56.53–67.86 Ma), consistent with the fossil record of *Styrax* [56,86]. We estimated that *Sinojackia* originated in the early Miocene (20.89 Ma, 95% HPD: 16.04–25.88 Ma), which is slightly later than the results of Rose et al. (22.1 Ma) [58] and Zhang et al. (24.0 Ma) [59]. The different selection of fossil calibration points and the slower nucleotide substitution rate of the plastome may produce inconsistent results. The diversification of *Sinojackia* was dated to the middle Miocene (14.50 Ma, 95% HPD: 7.01–21.33 Ma). Interspecific diversification in the genus *Sinojackia* mainly occurred in the later Miocene (4.69–9.44 Ma). The intraspecific diversity of *Sinojackia* mainly appeared in the Quaternary.

Some scholars believe that Southwest China may be a primitive differentiation center of the Styracaceae species and that *Sinojackia* might originate locally (Nanling Mountain Range, China) [87]. The diversification of Styracaceae corresponds to the Paleocene–Eocene Thermal Maximum (PETM) (55.8 Ma). During this period, there was an abrupt global warming caused by a transient burst of carbon dioxide [88,89]. This seems to indicate that the increase in temperature during the PETM causing the species diversity of Styracaceae. Subsequently, Styracaceae may have migrated from Southwestern China to Central and Southeastern China.

Sinojackia was initially differentiated after the Oligocene–Miocene (O–M) boundary (ca. 23 Ma) in central Southwestern China, when the modern East Asian flora began to rise [90]. The establishment and development of the Asian monsoon climate, accompanied by heavy rainfall, has led to species diversity in East Asian flora [90,91]. This also triggered a shift in Central and Southeastern China, leading to more the humid forest flora that are seen today [90]. In this process, new habitats may have appeared, which may have provided a suitable environment for the origin of *Sinojackia*. Furthermore, the global climate has become cooler since the middle Miocene, which has seriously affected the geographical structure pattern of plant lineages in the subtropical region of China [92]. Our molecular dating analyses indicate that *Sinojackia* initially diverged when a climatic cooling event occurred after the middle Miocene. This indicates that paleoclimatic events might have played a crucial role in the species differentiation and evolution of *Sinojackia*. With the development of the Asian monsoon, progressive global cooling, and the origin of East Asian flora, ancestral *Sinojackia* may have migrated from the Hubei Southeast China (C)

region to the Hunan Province and the Sichuan Province, evolving into *S. oblongicarpa* and *S. sarcocarpa*, respectively.

During the Quaternary, glacial–interglacial interactions with the monsoon climate played a crucial role in shaping plant diversity. Many plants experienced elevated diversification at intraspecies levels since this period [93]. Our molecular dating also demonstrates that *Sinojackia* experienced elevated diversification after the Quaternary. Subtropical (Central/South/East) China belongs to the Sino-Japanese Floristic Region (SJFR); this region was not covered by extensive glacial sheets during the Quaternary [94], and the impact of the ice age was much smaller here than that on the Qinghai Tibet Plateau and its adjacent areas. Thus, the subtropical China became a refuge for many plants during the glacial period. There are three ways for plants in subtropical China to respond to Quaternary climate fluctuations: glacial retreat and subsequent recolonization, in situ survival, and glacial expansion and interglacial contraction [95–97]. The species of *Sinojackia* are mainly distributed in low-altitude woodlands, so they are less affected by Quaternary climate shocks. Furthermore, several warm and long interglacial periods after the middle Pleistocene (1.2–0.8 Ma) provided favorable expansion conditions for plants in China [93]. Therefore, *Sinojackia* species may have experienced small-scale population expansion in situ during this period, and no long-distance migration occurred.

5. Conclusions

In this study, the plastomes of *S. oblongicarpa* were assembled and compared with those of other *Sinojackia* species. Little plastome structure and sequence variation was detected among the six *Sinojackia* species. Our phylogenetic tree indicated that *S. oblongicarpa* was close to (*S. xylocarpa* + *S. rehderiana*) and should be treated as an independent species. The taxonomic relationship between *S. rehderiana* and *S. xylocarpa* still needs to be reevaluated, and extensive taxon sampling and molecular characterization is essential to decipher the taxonomic delimitation and explore the evolutionary history of the two species. Our result demonstrated that mesocarp wood is probably an ancestral state of *Sinojackia*, and mesocarp undeveloped, spongy, and fleshy may be more evolved. Furthermore, climatic oscillation in the Miocene triggered speciation and migration in this genus.

Supplementary Materials: The following supporting information can be downloaded at <https://www.mdpi.com/article/10.3390/d16050305/s1>: Figure S1. Codon usage bias analyses of *S. sarcocarpa*; Figure S2. Codon usage bias analyses of *S. huangmeiensis*; Figure S3. Codon usage bias analyses of *S. macrocarpa*; Figure S4. Codon usage bias analyses of *S. rehderiana*; Figure S5. Codon usage bias analyses of *S. xylocarpa*.

Author Contributions: Funding acquisition, project administration, writing, and editing: Y.M.; data curation, software, supervision, writing—original draft, and validation: X.J., Q.L. and Y.W. All authors have read and agreed to the published version of the manuscript.

Funding: This research was funded by the Natural Science Research Project of Anhui Province University, grant number: 2023AH051882.

Institutional Review Board Statement: Not applicable.

Data Availability Statement: The plastomes have been deposited in GenBank under the accession numbers: OQ985171, OQ985172, and OQ985173. The raw data are available at SRA under the accession Nos. PRJNA1005030, PRJNA1005087, and PRJNA1006152.

Conflicts of Interest: The authors declare no conflicts of interest.

References

1. Schneider, J.; Döring, E.; Hilu, K.W.; Röser, M. Phylogenetic Structure of the Grass Subfamily Pooideae Based on Comparison of Plastid MatK Gene-3'trnK Exon and Nuclear ITS Sequences. *Taxon* **2009**, *58*, 405–424. [CrossRef]
2. Orton, L.M.; Barberá, P.; Nissenbaum, M.P.; Peterson, P.M.; Quintanar, A.; Soreng, R.J.; Duvall, M.R. A 313 Plastome Phylogenomic Analysis of Pooideae: Exploring Relationships among the Largest Subfamily of Grasses. *Mol. Phylogenet. Evol.* **2021**, *159*, 107110. [CrossRef] [PubMed]

3. Widmer, A.; Baltisberger, M. Extensive Intraspecific Chloroplast DNA (CpDNA) Variation in the Alpine *Draba aizoides* L. (Brassicaceae): Haplotype Relationships and Population Structure. *Mol. Ecol.* **1999**, *8*, 1405–1415. [[CrossRef](#)] [[PubMed](#)]
4. Huang, J.C.; Wang, W.K.; Peng, C.I.; Chiang, T.Y. Phylogeography and Conservation Genetics of *Hygrophila Pogonocalyx* (Acanthaceae) Based on AtpB-RbcL Noncoding Spacer CpDNA. *J. Plant Res.* **2005**, *118*, 1–11. [[CrossRef](#)] [[PubMed](#)]
5. Mayer, M.S.; Soltis, P.S. Intraspecific Phylogeny Analysis Using ITS Sequences: Insights from Studies of the *Streptanthus Glandulosus* Complex (Cruciferae). *Syst. Bot.* **1999**, *24*, 47–61. [[CrossRef](#)]
6. Zhao, L.; Zhang, N.; Ma, P.F.; Liu, Q.; Li, D.Z.; Guo, Z.H. Phylogenomic Analyses of Nuclear Genes Reveal the Evolutionary Relationships within the BEP Clade and the Evidence of Positive Selection in Poaceae. *PLoS ONE* **2013**, *8*, e64642. [[CrossRef](#)] [[PubMed](#)]
7. Burke, S.V.; Clark, L.G.; Triplett, J.K.; Grennan, C.P.; Duvall, M.R. Biogeography and Phylogenomics of New World Bambusoideae (Poaceae), Revisited. *Am. J. Bot.* **2014**, *101*, 886–891. [[CrossRef](#)] [[PubMed](#)]
8. Attigala, L.; Wysocki, W.P.; Duvall, M.R.; Clark, L.G. Phylogenetic Estimation and Morphological Evolution of Arundinarieae (Bambusoideae: Poaceae) Based on Plastome Phylogenomic Analysis. *Mol. Phylogenet. Evol.* **2016**, *101*, 111–121. [[CrossRef](#)]
9. Su, J.X.; Dong, C.C.; Niu, Y.T.; Lu, L.M.; Xu, C.; Liu, B.; Zhou, S.L.; Lu, A.M.; Zhu, Y.P.; Wen, J.; et al. Molecular Phylogeny and Species Delimitation of Stachyuraceae: Advocating a Herbarium Specimen-Based Phylogenomic Approach in Resolving Species Boundaries. *J. Syst. Evol.* **2020**, *58*, 710–724. [[CrossRef](#)]
10. Luo, Y.; He, J.; Lyu, R.; Xiao, J.; Li, W.; Yao, M.; Pei, L.; Cheng, J.; Li, J.; Xie, L. Comparative Analysis of Complete Chloroplast Genomes of 13 Species in *Epilobium*, *Circaea*, and *Chamaenerion* and Insights into Phylogenetic Relationships of Onagraceae. *Front. Genet.* **2021**, *12*, 730495. [[CrossRef](#)]
11. Namgung, J.; Do, H.D.K.; Kim, C.; Choi, H.J.; Kim, J.-H. Complete Chloroplast Genomes Shed Light on Phylogenetic Relationships, Divergence Time, and Biogeography of Allioideae (Amaryllidaceae). *Sci. Rep.* **2021**, *11*, 3262. [[CrossRef](#)] [[PubMed](#)]
12. Pereira, J.B.S.; Giulietti, A.M.; Prado, J.; Vasconcelos, S.; Watanabe, M.T.C.; Pinangé, D.S.B.; Oliveira, R.R.M.; Pires, E.S.; Caldeira, C.F.; Oliveira, G. Plastome-Based Phylogenomics Elucidate Relationships in Rare *Isoëtes* Species Groups from the Neotropics. *Mol. Phylogenet. Evol.* **2021**, *161*, 107177. [[CrossRef](#)] [[PubMed](#)]
13. Hwang, S.M.; Grimes, J. *Sinojackia*. In *Flora of China*; Wu, C.Y., Raven, P., Eds.; Science Press: Beijing, China; Missouri Botanical Garden Press: St. Louis, MO, USA, 1996; pp. 267–269.
14. Luo, L. A New Synonym in the Genus *Sinojackia* (Styracaceae). *Acta Phytotaxon. Sin.* **2005**, *43*, 561–564. [[CrossRef](#)]
15. Wang, Y.; Zhu, X.; Yang, Y.; Li, Z. New Taxa, Nomenclature, and Chromosome Report. *J. Syst. Evol.* **2011**, *49*, 160–164. [[CrossRef](#)]
16. Yao, X.H.; Ye, Q.G.; Ge, J.W.; Ming, K.; Huang, H.W. A New Species of *Sinojackia* (Styracaceae) from Hubei, Central China. *Novon* **2007**, *17*, 138–140. [[CrossRef](#)]
17. Zhang, J.; Ye, Q.; Gao, P.; Yao, X. Genetic Footprints of Habitat Fragmentation in the Extant Populations of *Sinojackia* (Styracaceae): Implications for Conservation. *Bot. J. Linn. Soc.* **2012**, *170*, 232–242. [[CrossRef](#)]
18. Tang, J.; Tang, R.; Chen, C. Cultivation Technology and Application of *Sinojackia*. *Contemp. Hortic.* **2015**, *294*, 49–50. [[CrossRef](#)]
19. Liu, S.; Zhou, Z. Study on the Bacteriostatic Action of the Extracts from the Leaves of *Sinojackia sarcocarpa*. *J. Anhui Agri. Sci.* **2008**, *36*, 9599–9600. [[CrossRef](#)]
20. Zhong, T.; Zhuo, J.; Chen, D.; Vasupalli, N.; Chu, J.; Qian, Q. Complete Chloroplast Genome Sequence of *Sinojackia microcarpa* (Styracaceae): Comparative and Phylogenetic Analysis. *Biologia* **2021**, *76*, 3891–3900. [[CrossRef](#)]
21. Fu, L.K.; Jin, J.M. *China Plant Red Data Book—Rare and Endangered Plants*; Science Press: Beijing, China, 1992.
22. Wang, S.; Xie, Y. *China Species Red List*; Higher Education Press: Beijing, China, 2004.
23. Yao, X. Geographic Distribution and Current Status of the Endangered Genera *Sinojackia* and *Changiostyrax*. *Biodivers. Sci.* **2005**, *13*, 339. [[CrossRef](#)]
24. Hu, H.H. *Sinojackia*, a New Genus of Styracaceae from Southeastern China. *J. Arnold Arbor.* **1928**, *9*, 130–131. [[CrossRef](#)]
25. Qi, C. A New Species of Styracaceae from Hunan. *Acta Phytotaxon. Sin.* **1981**, *19*, 526–528.
26. Chen, T.; Li, G. A New Species of *Sinojackia* Hu (Styracaceae) from Zhejiang, East China. *Novon* **1997**, *7*, 350–352. [[CrossRef](#)]
27. Chen, T.; Cao, T. A New Species of *Sinojackia* Hu (Styracaceae) from Hunan, South Central China. *Edinb. J. Bot.* **1998**, *55*, 235–238. [[CrossRef](#)]
28. Hu, H.H. Notulae Systematicae Ad Floram Sinensem, II. *J. Arnold Arbor.* **1930**, *11*, 224–228. [[CrossRef](#)]
29. Luo, L. A New Species of *Sinojackia* from Sichuan. *Acta Sci. Nat. Univ. Sunyatseni* **1992**, *31*, 78–79.
30. Luo, L. *Sinojackia xylocarpa* var. *leshanensis* (Styracaceae) a New Variety from Sichuan, China. *Bull. Bot. Res.* **2005**, *25*, 260–261.
31. Merrill, E.D. *Miscellanea Sinensia. Sunyatsenia* **1937**, *3*, 246–262.
32. Yao, X.; Ye, Q.; Fritsch, P.W.; Cruz, B.C.; Huang, H. Phylogeny of *Sinojackia* (Styracaceae) Based on DNA Sequence and Microsatellite Data: Implications for Taxonomy and Conservation. *Ann. Bot.* **2008**, *101*, 651–659. [[CrossRef](#)]
33. Chen, T. *Changiostyrax*, a New Genus of Styracaceae from China. *Guihaia* **1995**, *15*, 289–292.
34. Fritsch, P.W. Phylogeny and Biogeography of the Flowering Plant Genus *Styrax* (Styracaceae) Based on Chloroplast DNA Restriction Sites and DNA Sequences of the Internal Transcribed Spacer Region. *Mol. Phylogenet. Evol.* **2001**, *19*, 387–408. [[CrossRef](#)] [[PubMed](#)]
35. Yan, M.; Fritsch, P.W.; Moore, M.J.; Feng, T.; Meng, A.; Yang, J.; Deng, T.; Zhao, C.; Yao, X.; Sun, H.; et al. Plastid Phylogenomics Resolves Intrafamilial Relationships of the Styracaceae and Sheds Light on the Backbone Relationships of the Ericales. *Mol. Phylogenet. Evol.* **2018**, *121*, 198–211. [[CrossRef](#)] [[PubMed](#)]

36. Cai, X.L.; Landis, J.B.; Wang, H.X.; Wang, J.H.; Zhu, Z.X.; Wang, H.F. Plastome Structure and Phylogenetic Relationships of Styracaceae (Ericales). *BMC Ecol. Evol.* **2021**, *21*, 103. [[CrossRef](#)] [[PubMed](#)]
37. Fan, J.; Luo, Y.; Huang, M.; Liang, Z.; Chen, H.; Wu, M. Analysis of RDNA-ITS Molecular Identification, Seed Morphology and Breeding on the Endangered *Sinojackia sarcocarpa* in Sichuan. *Genom. Appl. Biol.* **2015**, *34*, 2483–2491. [[CrossRef](#)]
38. Dong, H.; Wang, H.; Li, Y.; Yu, J. The Complete Chloroplast Genome Sequence of *Sinojackia huangmeiensis* (Styracaceae). *Mitochondrial DNA Part B Resour.* **2020**, *5*, 715–717. [[CrossRef](#)] [[PubMed](#)]
39. Fan, J.; Fu, Q.C.; Liang, Z. Complete Chloroplast Genome Sequence and Phylogenetic Analysis of *Sinojackia sarcocarpa*, an Endemic Plant in Southwest China. *Mitochondrial DNA Part B Resour.* **2019**, *4*, 1350–1351. [[CrossRef](#)]
40. Doyle, J.J.; Doyle, J.L. Genomic Plant DNA Preparation from Fresh Tissue-CTAB Method. *Phytochem. Bull.* **1987**, *19*, 11–15.
41. Chen, S.; Zhou, Y.; Chen, Y.; Gu, J. Fastp: An Ultra-Fast All-in-One FASTQ Preprocessor. *Bioinformatics* **2018**, *34*, i884–i890. [[CrossRef](#)]
42. Jin, J.J.; Wen, B.Y.; Yang, J.B.; Song, Y.; Depamphilis, C.W.; Yi, T.S.; Li, D.Z. GetOrganelle: A Fast and Versatile Toolkit for Accurate de Novo Assembly of Organelle Genomes. *Genome Biol.* **2020**, *21*, 241. [[CrossRef](#)]
43. Wick, R.R.; Schultz, M.B.; Zobel, J.; Holt, K.E. Bandage: Interactive Visualization of de Novo Genome Assemblies. *Bioinformatics* **2015**, *31*, 3350–3352. [[CrossRef](#)]
44. Shi, L.; Chen, H.; Jiang, M.; Wang, L.; Wu, X.; Huang, L.; Liu, C. CPGAVAS2, an Integrated Plastome Sequence Annotator and Analyzer. *Nucleic Acids Res.* **2019**, *47*, W65–W73. [[CrossRef](#)] [[PubMed](#)]
45. Tillich, M.; Lehwark, P.; Pellizzer, T.; Ulbricht-Jones, E.S.; Fischer, A.; Bock, R.; Greiner, S. GeSeq—Versatile and Accurate Annotation of Organelle Genomes. *Nucleic Acids Res.* **2017**, *45*, W6–W11. [[CrossRef](#)] [[PubMed](#)]
46. Greiner, S.; Lehwark, P.; Bock, R. OrganellarGenomeDRAW (OGDRAW) Version 1.3.1: Expanded Toolkit for the Graphical Visualization of Organellar Genomes. *Nucleic Acids Res.* **2019**, *47*, W59–W64. [[CrossRef](#)] [[PubMed](#)]
47. Katoh, K.; Rozewicki, J.; Yamada, K.D. MAFFT Online Service: Multiple Sequence Alignment, Interactive Sequence Choice and Visualization. *Brief. Bioinform.* **2018**, *20*, 1160–1166. [[CrossRef](#)] [[PubMed](#)]
48. Rozas, J.; Ferrer-Mata, A.; Sanchez-DelBarrio, J.C.; Guirao-Rico, S.; Librado, P.; Ramos-Onsins, S.E.; Sanchez-Gracia, A. DnaSP 6: DNA Sequence Polymorphism Analysis of Large Data Sets. *Mol. Biol. Evol.* **2017**, *34*, 3299–3302. [[CrossRef](#)] [[PubMed](#)]
49. He, Z.; Gan, H.; Liang, X. Analysis of Synonymous Codon Usage Bias in Potato Virus M and Its Adaptation to Hosts. *Viruses* **2019**, *11*, 752. [[CrossRef](#)] [[PubMed](#)]
50. Guan, D.-L.; Ma, L.-B.; Khan, M.S.; Zhang, X.-X.; Xu, S.-Q.; Xie, J.-Y. Analysis of Codon Usage Patterns in *Hirudinaria manillensis* Reveals a Preference for GC-Ending Codons Caused by Dominant Selection Constraints. *BMC Genom.* **2018**, *19*, 542. [[CrossRef](#)] [[PubMed](#)]
51. Yang, G.; Su, K.; Zhao, Y.; Song, Z.; Sun, J. Analysis of Codon Usage in the Chloroplast Genome of *Medicago truncatula*. *Acta Prataculturae Sin.* **2015**, *24*, 171–179.
52. Yu, X.; Liu, J.; Li, H.; Liu, B.; Zhao, B.; Ning, Z. Comprehensive Analysis of Synonymous Codon Usage Patterns and Influencing Factors of Porcine Epidemic Diarrhea Virus. *Arch. Virol.* **2021**, *166*, 157–165. [[CrossRef](#)]
53. Zhang, D.; Gao, F.; Jakovlić, I.; Zou, H.; Zhang, J.; Li, W.X.; Wang, G.T. PhyloSuite: An Integrated and Scalable Desktop Platform for Streamlined Molecular Sequence Data Management and Evolutionary Phylogenetics Studies. *Mol. Ecol. Resour.* **2020**, *20*, 348–355. [[CrossRef](#)]
54. Minh, B.Q.; Schmidt, H.A.; Chernomor, O.; Schrempf, D.; Woodhams, M.D.; Von Haeseler, A.; Lanfear, R.; Teeling, E. IQ-TREE 2: New Models and Efficient Methods for Phylogenetic Inference in the Genomic Era. *Mol. Biol. Evol.* **2020**, *37*, 1530–1534. [[CrossRef](#)] [[PubMed](#)]
55. Bouckaert, R.; Heled, J.; Kühnert, D.; Vaughan, T.; Wu, C.H.; Xie, D.; Suchard, M.A.; Rambaut, A.; Drummond, A.J. BEAST 2: A Software Platform for Bayesian Evolutionary Analysis. *PLoS Comput. Biol.* **2014**, *10*, e1003537. [[CrossRef](#)] [[PubMed](#)]
56. Chandler, M.E.J. *The Lower Tertiary Floras of Southern England: Flora of the Pipe-Clay Series of Dorset (Lower Bagshot)*; British Museum (Natural History): London, UK, 1962; Volume 2.
57. MacGinitie, H.D. *Fossil Plants of the Florissant Beds, Colorado*; Carnegie Institution of Washington: Washington, DC, USA, 1953.
58. Rose, J.P.; Kleist, T.J.; Löfstrand, S.D.; Drew, B.T.; Schönenberger, J.; Sytsma, K.J. Phylogeny, Historical Biogeography, and Diversification of Angiosperm Order Ericales Suggest Ancient Neotropical and East Asian Connections. *Mol. Phylogenet. Evol.* **2018**, *122*, 59–79. [[CrossRef](#)] [[PubMed](#)]
59. Zhang, C.; Zhang, T.; Luebert, F.; Xiang, Y.; Huang, C.; Hu, Y.; Rees, M.; Frohlich, M.W.; Qi, J.; Weigend, M.; et al. Asterid Phylogenomics/Phylotranscriptomics Uncover Morphological Evolutionary Histories and Support Phylogenetic Placement for Numerous Whole-Genome Duplications. *Mol. Biol. Evol.* **2020**, *37*, 3188–3210. [[CrossRef](#)] [[PubMed](#)]
60. Xu, S.; Ma, D.; Zhang, F.; Xu, L.; Li, X.; Chen, Z. A New Record Species of Styracaceae from Zhejiang Province. *J. Zhejiang For. Sci. Technol.* **2022**, *42*, 61–64. [[CrossRef](#)]
61. Yu, Y.; Blair, C.; He, X. RASP 4: Ancestral State Reconstruction Tool for Multiple Genes and Characters. *Mol. Biol. Evol.* **2020**, *37*, 604–606. [[CrossRef](#)] [[PubMed](#)]
62. Ishikawa, S.A.; Zhukova, A.; Iwasaki, W.; Gascuel, O.; Pupko, T. A Fast Likelihood Method to Reconstruct and Visualize Ancestral Scenarios. *Mol. Biol. Evol.* **2019**, *36*, 2069–2085. [[CrossRef](#)] [[PubMed](#)]
63. Feng, Y.; Gao, X.-F.; Zhang, J.-Y.; Jiang, L.-S.; Li, X.; Deng, H.-N.; Liao, M.; Xu, B. Complete Chloroplast Genomes Provide Insights into Evolution and Phylogeny of *Campylotropis* (Fabaceae). *Front. Plant Sci.* **2022**, *13*, 895543. [[CrossRef](#)] [[PubMed](#)]

64. Xu, S.; Teng, K.; Zhang, H.; Gao, K.; Wu, J.; Duan, L.; Yue, Y.; Fan, X. Chloroplast Genomes of Four *Carex* Species: Long Repetitive Sequences Trigger Dramatic Changes in Chloroplast Genome Structure. *Front. Plant Sci.* **2023**, *14*, 1100876. [[CrossRef](#)]
65. Wang, L.; Li, Y.; He, N.; Peng, Y.; Fang, Y.; Zhang, X.; Zhang, F. Comparative Chloroplast Genome Analysis of Chinese Lacquer Tree (*Toxicodendron vernicifluum*, Anacardiaceae): East-West Divergence within Its Range in China. *Forests* **2023**, *14*, 818. [[CrossRef](#)]
66. Li, Q. The Complete Chloroplast Genomes of *Primula obconica* Provide Insight That Neither Species nor Natural Section Represent Monophyletic Taxa in *Primula* (Primulaceae). *Genes* **2022**, *13*, 567. [[CrossRef](#)]
67. Chen, Z.; Grover, C.E.; Li, P.; Wang, Y.; Nie, H.; Zhao, Y.; Wang, M.; Liu, F.; Zhou, Z.; Wang, X.; et al. Molecular Evolution of the Plastid Genome during Diversification of the Cotton Genus. *Mol. Phylogenet. Evol.* **2017**, *112*, 268–276. [[CrossRef](#)]
68. Mohanta, T.K.; Mishra, A.K.; Khan, A.; Hashem, A.; Abd-Allah, E.F.; Al-Harrasi, A. Gene Loss and Evolution of the Plastome. *Genes* **2020**, *11*, 1133. [[CrossRef](#)] [[PubMed](#)]
69. Zhao, K.; Li, L.; Quan, H.; Yang, J.; Zhang, Z.; Liao, Z.; Lan, X. Comparative Analyses of Chloroplast Genomes from Six *Rhodiola* Species: Variable DNA Markers Identification and Phylogenetic Relationships within the Genus. *BMC Genom.* **2022**, *23*, 577. [[CrossRef](#)] [[PubMed](#)]
70. Salim, H.M.W.; Cavalcanti, A.R.O. Factors Influencing Codon Usage Bias in Genomes. *J. Braz. Chem. Soc.* **2008**, *19*, 257–262. [[CrossRef](#)]
71. Parvathy, S.T.; Udayasuriyan, V.; Bhadana, V. Codon Usage Bias. *Mol. Biol. Rep.* **2022**, *49*, 539–565. [[CrossRef](#)] [[PubMed](#)]
72. Zhang, Y.; Shen, Z.; Meng, X.; Zhang, L.; Liu, Z.; Liu, M.; Zhang, F.; Zhao, J. Codon Usage Patterns across Seven Rosales Species. *BMC Plant Biol.* **2022**, *22*, 65. [[CrossRef](#)] [[PubMed](#)]
73. Wang, Y.; Jiang, D.; Guo, K.; Zhao, L.; Meng, F.; Xiao, J.; Niu, Y.; Sun, Y. Comparative Analysis of Codon Usage Patterns in Chloroplast Genomes of Ten *Epimedium* Species. *BMC Genom. Data* **2023**, *24*, 3. [[CrossRef](#)] [[PubMed](#)]
74. Morton, B.R. The Role of Context-Dependent Mutations in Generating Compositional and Codon Usage Bias in Grass Chloroplast DNA. *J. Mol. Evol.* **2003**, *56*, 616–629. [[CrossRef](#)]
75. Quax, T.E.F.; Claassens, N.J.; Söll, D.; van der Oost, J. Codon Bias as a Means to Fine-Tune Gene Expression. *Mol. Cell* **2015**, *59*, 149–161. [[CrossRef](#)]
76. Chen, S.L.; Lee, W.; Hottes, A.K.; Shapiro, L.; McAdams, H.H. Codon Usage between Genomes Is Constrained Genome-Wide Mutational Processes. *Proc. Natl. Acad. Sci. USA* **2004**, *101*, 3480–3485. [[CrossRef](#)] [[PubMed](#)]
77. Liu, Y. A Code within the Genetic Code: Codon Usage Regulates Co-Translational Protein Folding. *Cell Commun. Signal.* **2020**, *18*, 145. [[CrossRef](#)] [[PubMed](#)]
78. Shi, S.-L.; Liu, Y.-Q.; Xia, R.-X.; Qin, L. Comprehensive Analysis of Codon Usage in *Quercus* Chloroplast Genome and Focus on *PsbA* Gene. *Genes* **2022**, *13*, 2156. [[CrossRef](#)] [[PubMed](#)]
79. Nair, R.R.; Nandhini, M.B.; Monalisha, E.; Murugan, K.; Nagarajan, S.; Surya, N.; Rao, P.; Ganesh, D. Synonymous Codon Usage in Chloroplast Genome of *Coffea arabica*. *Bioinformatics* **2012**, *8*, 1096–1104. [[CrossRef](#)] [[PubMed](#)]
80. Zhang, P.; Xu, W.; Lu, X.; Wang, L. Analysis of Codon Usage Bias of Chloroplast Genomes in *Gynostemma* Species. *Physiol. Mol. Biol. Plants* **2021**, *27*, 2727–2737. [[CrossRef](#)] [[PubMed](#)]
81. Zhang, J.J.; Ye, Q.G.; Yao, X.H.; Huang, H.W. Spontaneous Interspecific Hybridization and Patterns of Pollen Dispersal in Ex Situ Populations of a Tree Species (*Sinojackia xylocarpa*) That Is Extinct in the Wild: Contributed Paper. *Conserv. Biol.* **2010**, *24*, 246–255. [[CrossRef](#)]
82. Quan, J.; Xu, Z.; Kang, Z.; Yang, Z.; Luozhong, T. Basic Characteristic and Dormancy Mechanism of *Sinojackia xylocarpa* Fruit and Seed. *J. Southwest For. Univ.* **2021**, *41*, 145–150.
83. Wu, Y.; Bao, W.Q.; Hu, H.; Shen, Y.B. Mechanical Constraints in the Endosperm and Endocarp Are Major Causes of Dormancy in *Sinojackia xylocarpa* Hu (Styracaceae) Seeds. *J. Plant Growth Regul.* **2023**, *42*, 644–657. [[CrossRef](#)]
84. Dexter, K.; Chave, J. Evolutionary Patterns of Range Size, Abundance and Species Richness in Amazonian Angiosperm Trees. *PeerJ* **2016**, *2016*, e2402. [[CrossRef](#)]
85. Li, H.T.; Yi, T.S.; Gao, L.M.; Ma, P.F.; Zhang, T.; Yang, J.B.; Gitzendanner, M.A.; Fritsch, P.W.; Cai, J.; Luo, Y.; et al. Origin of Angiosperms and the Puzzle of the Jurassic Gap. *Nat. Plants* **2019**, *5*, 461–470. [[CrossRef](#)]
86. Ozaki, K. Late Miocene and Pliocene Floras in Central Honshu, Japan. *Bull. Kanagawa Prefect. Museum Nat. Sci. Special Issue.* **1991**, 1–244.
87. Chen, T.; Chen, Z. The Geographical Distribution of Styracaceae. *Bull. Bot. Res.* **1996**, *16*, 57–66.
88. Currano, E.D.; Wilf, P.; Wing, S.L.; Labandeira, C.C.; Lovelock, E.C.; Royer, D.L. Sharply Increased Insect Herbivory during the Paleocene-Eocene Thermal Maximum. *Proc. Natl. Acad. Sci. USA* **2008**, *105*, 1960–1964. [[CrossRef](#)] [[PubMed](#)]
89. McInerney, F.A.; Wing, S.L. The Paleocene-Eocene Thermal Maximum: A Perturbation of Carbon Cycle, Climate, and Biosphere with Implications for the Future. *Annu. Rev. Earth Planet. Sci.* **2011**, *39*, 489–516. [[CrossRef](#)]
90. Chen, Y.S.; Deng, T.; Zhou, Z.; Sun, H. Is the East Asian Flora Ancient or Not? *Natl. Sci. Rev.* **2018**, *5*, 920–932. [[CrossRef](#)]
91. Li, S.F.; Valdes, P.J.; Farnsworth, A.; Davies-Barnard, T.; Su, T.; Lunt, D.J.; Spicer, R.A.; Liu, J.; Deng, W.Y.D.; Huang, J.; et al. Orographic Evolution of Northern Tibet Shaped Vegetation and Plant Diversity in Eastern Asia. *Sci. Adv.* **2021**, *7*, eabc7741. [[CrossRef](#)] [[PubMed](#)]
92. Ye, J.W.; Zhang, Y.; Wang, X.J. Phylogeographic History of Broad-Leaved Forest Plants in Subtropical China. *Acta Ecol. Sin.* **2017**, *37*, 5894–5904. [[CrossRef](#)]

93. Kou, Y.; Cheng, S.; Tian, S.; Li, B.; Fan, D.; Chen, Y.; Soltis, D.E.; Soltis, P.S.; Zhang, Z. The Antiquity of *Cyclocarya paliurus* (Juglandaceae) Provides New Insights into the Evolution of Relict Plants in Subtropical China since the Late Early Miocene. *J. Biogeogr.* **2016**, *43*, 351–360. [[CrossRef](#)]
94. Gong, W.; Chen, C.; Dobeš, C.; Fu, C.X.; Koch, M.A. Phylogeography of a Living Fossil: Pleistocene Glaciations Forced *Ginkgo biloba* L. (Ginkgoaceae) into Two Refuge Areas in China with Limited Subsequent Postglacial Expansion. *Mol. Phylogenet. Evol.* **2008**, *48*, 1094–1105. [[CrossRef](#)]
95. Li, X.H.; Shao, J.W.; Lu, C.; Zhang, X.P.; Qiu, Y.X. Chloroplast Phylogeography of a Temperate Tree *Pteroceltis tatarinowii* (Ulmaceae) in China. *J. Syst. Evol.* **2012**, *50*, 325–333. [[CrossRef](#)]
96. Wang, Y.H.; Comes, H.P.; Cao, Y.N.; Guo, R.; Mao, Y.R.; Qiu, Y.X. Quaternary Climate Change Drives Allo-Peripatric Speciation and Refugial Divergence in the *Dysosma versipellis-pleiantha* Complex from Different Forest Types in China. *Sci. Rep.* **2017**, *7*, 40261. [[CrossRef](#)] [[PubMed](#)]
97. Lu, R.-S.; Chen, Y.; Tamaki, I.; Sakaguchi, S.; Ding, Y.-Q.; Takahashi, D.; Li, P.; Isaji, Y.; Chen, J.; Qiu, Y.-X. Pre-Quaternary Diversification and Glacial Demographic Expansions of *Cardiocrinum* (Liliaceae) in Temperate Forest Biomes of Sino-Japanese Floristic Region. *Mol. Phylogenet. Evol.* **2020**, *143*, 106693. [[CrossRef](#)] [[PubMed](#)]

Disclaimer/Publisher’s Note: The statements, opinions and data contained in all publications are solely those of the individual author(s) and contributor(s) and not of MDPI and/or the editor(s). MDPI and/or the editor(s) disclaim responsibility for any injury to people or property resulting from any ideas, methods, instructions or products referred to in the content.